Separating Catalytic Activity at Edges and Terraces on Platinum: Hydrogen Dissociation
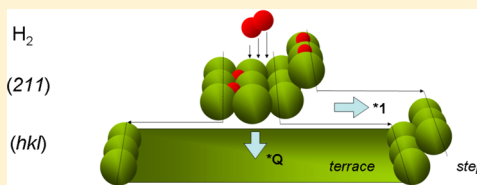
I. M. N. Groot,[†,‡] A. W. Kleyn,[†,‡,§] and L. B. F. Juurlink*,[†]

[†]Leiden Institute of Chemistry, Leiden University, P.O. BOX 9502, 2300 RA Leiden, The Netherlands
[‡]FOM Institute DIFFER, P.O. Box 1207, 3430 BE Nieuwegein, The Netherlands
[§]Van't Hoff Institute for Molecular Sciences, University of Amsterdam, P.O. Box 94157, 1090 GD Amsterdam, The Netherlands

ABSTRACT: Heterogeneous catalysis relies to a large extent on the reactivity of metal nanoparticles. The surface of these particles consists of atomically smooth terraces and edges. As local environments of atoms in edges and terraces are different, their catalytic ability varies. This severely complicates accurate predictions of reaction kinetics in heterogeneous catalysis. In this study, we use the reaction dynamics of H_2 dissociation on a series of $[n(111) \times (100)]$ stepped platinum single-crystal surfaces to resolve how reactivity for atoms in edges and terraces can be separated and quantified individually. A simple reactivity model that only requires input from $n = 3$ accurately predicts reactivity for any combination of a (100) step with a (111) terrace over the entire energy range of interest for incident molecules. Our results support the assumption in theoretical kinetics studies that the smallest unit cell accurately models the essential features of the catalytic surface, and we discuss limitations to this assumption. Finally, from our model, we quantify for the first time the absolute reaction cross section for a direct dissociative process in a gas–surface collision.

INTRODUCTION

Metallic nanoparticles used in heterogeneous catalysis are often at most 20 nm in diameter. Figure 1 illustrates how the atoms
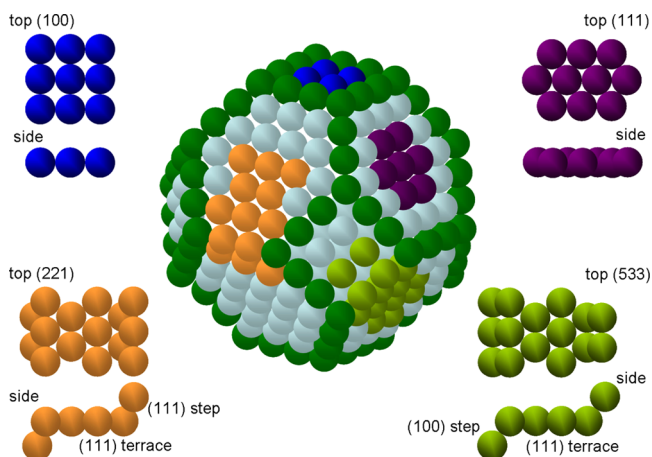

Figure 1. Idealized catalytic particle for a face-centered cubic metal exhibiting (111) and (100) terraces. Top and side views of small sections of single-crystal surfaces as used in surface science studies surround the particle.

at the surface of an idealized catalytic particle form corners, edges, and terraces. Chemical reactions occur on different parts of the surface to varying degrees as the atoms making up these corners, edges, and terraces have different local environments and consequently different abilities to break chemical bonds, stabilize intermediates, or release products.

For several decades, macroscopic single-crystal surfaces have been used as models for catalytic particles in studies of heterogeneously catalyzed reaction mechanisms.[1,2] Originally, single crystals exposing a low Miller-index surface, for example, the (111) and (100) planes exhibited in Figure 1, with very large atomically flat terraces, received the most interest. However, it was quickly appreciated that regularly stepped surfaces, for example, the (533) and (221) surfaces also shown in Figure 1, provide means to study the reactivity of lower-coordinated surface atoms. Such surfaces contain edges or corners strongly resembling those on catalytic particles. Somorjai and co-workers pioneered the study of reactivity of stepped surfaces using the H−D exchange reaction.[3−7] They showed that the sum of elementary reaction steps leading to HD formation on platinum from impinging H_2 and D_2 depends on the surface's step density and the approach geometry of the reactants. When molecules impinged onto the open side of the step, HD formation was higher than when molecules impinged mostly on flat terraces. Although it clearly illustrated the higher reactivity of steps for H−D exchange, the extent to which step edges dominate overall reactivity in a more general sense is still lively debated.[8,9]

In the last decades, density functional theory (DFT) has provided a solid background to understanding general trends in heterogeneous catalysis. The *d*-band model, scaling relations between adsorption energies, and the Brønsted−Evans−Polanyi relations, relating adsorption energy and transition-state energy, are providing means to rationally design better catalysts from fundamental principles.[10] In such DFT-based

studies, it is also generally found that, compared to a flat surface, an atomic step alters the activation barrier for dissociation of a gas-phase reactant.[11] For computational reasons, these studies are often limited to the smallest possible unit cell containing a particular type of step. For example, the (211) surface, also indicated as $[3(111) \times (100)]$ in the microfacet notation proposed by Vanhove and Somorjai,[12] provides for face-centered cubic (fcc) metals the smallest unit cell containing a (111) terrace and a monoatomically high (100) step.

For predicting the chemical kinetics of heterogeneously catalyzed reactions based on first principles, the current level of accuracy is limited. Only when overall reactivity may safely be ascribed to a single rate-determining step occurring at a single type of site, this task is currently feasible. The production of NH_3 over a Ru catalyst seems to be such a case. Predictions of total reaction rates relying on DFT-based energy barriers for N_2 dissociation at a step site and a microkinetic model compare well to experimental data.[13,14] For other reactions that also rely on relatively high reactivity of a particular step site, for example, methane steam reforming[15] and HCN production from CH_4 and NH_3,[16] catalytic trends across transition metals are reproduced in agreement with measurements. However, quantitative comparison to experimental data seems not (yet) feasible.

In this paper, we show that reaction dynamics experiments can accurately discriminate between the reactivity of a step and a terrace site. As a model system, we use the dissociation of H_2 (D_2) on $Pt[n(111) \times (100)]$ surfaces. The general structure of such surfaces is indicated in the top half of Figure 2. Whereas

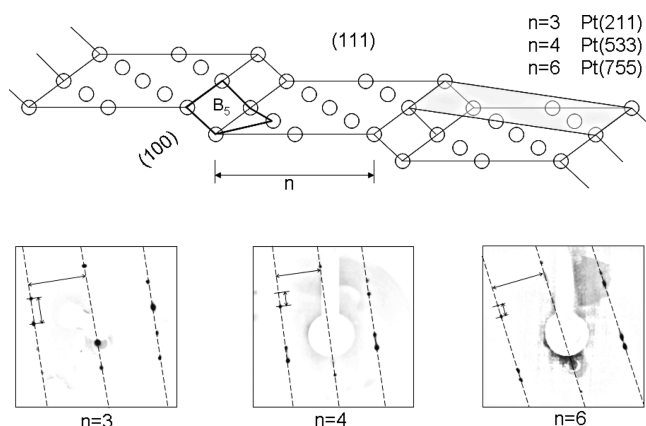**Figure 2.** (top) Schematic of the $Pt[n(111) \times (100)]$ with $n = 5$ surface. Also indicated are a B_5 site (thick lines) and unit cell (gray shaded area) (bottom) low-energy electron diffraction images of surfaces with n = 3, 4, and 6. Arrowed lines indicate spot-splitting and row-spacing distances.

the terrace is composed of hexagonally arranged atoms, the step is formed by a square arrangement. This particular geometry creates, independent of terrace length, a "cradle" composed of five atoms at the step that is also referred to as a B_5 site. Van Hardeveld and van Montfoort introduced this site nomenclature with their suggestion that the two possible variations of this type of site were responsible for anomalously strong binding of N_2 to Ni, Pd and Pt catalysts.[17] For an fcc metal surface with (111) terraces, the two variations of B_5 sites consist of a combination of a 4-fold and 3-fold sites in the case of a (100) step or two 3-fold hollows for a (110) step. The first of

these two variations is considered the only one to contribute significantly to the overall reactivity in the combined DFT–kinetics studies that accurately predicted formation of NH_3 over Ru-based catalysts.[13,14]

In the study presented here, we focus mostly on the initial elementary reaction step, that is, breaking of the H–H (D–D) bond, producing two surface-bound H (D) atoms. This elementary reaction has been studied in detail by theoretical[18,19] and experimental[20,21] means and therefore provides a good reference for our measurements. Theoretical dynamics studies on the most accurate potential energy surface (PES) for the (211) unit cell, that is, the smallest unit cell containing a (100) step and (111) terrace with n = 3, have suggested that H_2 dissociates via three different mechanisms.[18] First, nonactivated direct dissociation occurs when the impinging molecule hits the upper edge of a step. Reactivity for this mechanism is expected to be (mostly) energy-independent. Second, nonactivated indirect dissociation occurs when the molecule gently impinges near the lower edge of the step. This mechanism is induced by the presence of shallow molecular chemisorption wells at the bottom of the steps. Accommodation in these wells leads to dissociation at the upper edge of the step via a molecular precursor state.[18] As the kinetic energy of the impinging molecule needs to be absorbed or transformed to be accommodated initially, this mechanism's contribution rapidly decreases with increasing kinetic energy. Finally, direct activated dissociation occurs at the n-atom long terrace. The same mechanism is responsible for dissociation on Pt(111) where minimum energy barrier heights of 6, 25, and 40 kJ/mol are found for dissociation at top, bridge, and fcc sites.[22] This barrier height distribution results experimentally in a nearly linear increase in reaction probability with increasing kinetic energy and the observed (near-)normal energy scaling.[23,24] Poelsema, Lenz, and Comsa have recently suggested an additional dissociation mechanism through a nonaccommodated molecular precursor state on large terraces on clean and "defect free" Pt(111).[25,26] They also investigated the role of defects using adsorption from thermalized gas.[25,26] We comment on the relation between their model and our current work in the Results and Discussion section.

As dissociative adsorption of hydrogen on stepped surfaces is possible at various locations through different mechanisms with modest variations in activation barrier heights, the kinetic description of hydrogenation and H–D exchange reactions should take all possible dissociation pathways into account. This makes H_2/Pt a different type of model system compared to those where large discrepancies exist between dissociation at, for example, step and terrace sites. In the absence of additional "high-barrier" processes in the complete reaction mechanism, the kinetic description of the latter case may be simplified by introduction of a single rate-determining step for dissociative adsorption of a reactant. However, it is unlikely that the same simplification holds for all catalytic reactions.

Here, results from supersonic molecular beam studies on three difference planes (n = 3, 4, and 6) are compared to all other experimental results published to date. They show remarkable quantitative agreement, even for the comparison of results from different laboratories. Angle and kinetic energy dependencies of the reaction probability follow the trends predicted by theoretical studies. Modeling of the reaction probability data based on three different dissociation pathways allows us to extract physical parameters previously unattainable. We present how our model yields an absolute reaction cross

section for one of the three incorporated pathways leading to dissociation. In addition, we show that a simple predictive model using input from experimental data for $n = 3$ accurately predicts the kinetic energy dependence for any other value of n. This enables the construction of kinetic models that incorporate dynamical dependencies and multiple parallel pathways in dissociative adsorption as part of heterogeneously catalyzed reactions.

■ EXPERIMENTAL APPARATUS AND METHODS

Experiments were performed in a vacuum system that consists of five chambers individually pumped by turbomolecular pumps.[27] A supersonic expansion of pure or seeded H_2 (99.9999%) or D_2 (99.8%) from ~1–4 atm exits a 43 or 60 μm nozzle into the first chamber. A well-defined supersonic molecular beam is created by a series of skimmers and orifices and enters into the main ultrahigh vacuum (UHV) chamber (base pressure $<10^{-10}$ mbar). This chamber contains for every set of experiments one of a series of stepped Pt single-crystal surfaces, cut from the same boule (99.9995%) to within 0.1° of the (211), (533), and (755) faces, respectively (Surface Preparation Laboratory, Zaandam, The Netherlands). The crystals are all 10 mm in diameter and ~1 mm thick. The surfaces were polished using identical procedures prior to being introduced into the vacuum system. All surfaces were subsequently cleaned under UHV conditions using at least 50–100 extensive Ar^+ sputtering and annealing cycles prior to initiating experiments.

During experiments, daily cleaning procedures consist of repeated cycles of Ar^+ bombardment, followed by annealing in 2×10^{-8} mbar O_2 at 900 K to remove carbon and sulfur impurities. Subsequent annealing at 1200 K removes remaining O_2 and restores surface order. We test for surface quality by low-energy electron diffraction (LEED) and temperature-programmed desorption (TPD) spectroscopy of CO, NO, H_2, D_2, and O_2. TPD features are known to be very sensitive to impurities and cleanliness of the steps.[28−34] Cleaning cycles are repeated until no evidence for impurities is found and clear LEED images appear. From the split pattern of the LEED spots,[35,36] we determine the average terrace widths to be 2.9, 4.0, and 5.9 atoms wide, which is in agreement with the expectation of 3, 4, and 6 atom wide terraces, respectively, for Pt(211), Pt(533), and Pt(755). Typical LEED patterns observed for our three single-crystal surfaces are shown in the bottom half of Figure 2. Dotted lines are drawn through the spot rows. Double arrowed lines indicate spot-splitting and row-spacing distances.

The kinetic energy of the hydrogen molecules is controlled by both the temperature of the nozzle (300−1700 K) and (anti)seeding techniques of H_2 in Ar, N_2, and He and D_2 in Ar, N_2, and H_2. We determine the kinetic energy of H_2 and D_2 for all expansion conditions using time-of-flight (TOF) spectrometry. We can determine the kinetic energy in two different ways, one by fitting the TOF spectra to an appropriate form of the Boltzmann distribution (for details see ref 21), or by moving the differentially pumped quadrupole mass spectrometer (QMS) over a length of 175 mm and recording TOF spectra at different distances. The velocity of the expansion is then determined by plotting the additional distance versus additional flight time and determining the slope of the data.

The initial dissociation probability (S_0) is determined using the King and Wells technique.[37] For angle-dependence studies, the maximum incident angle is limited by the sizes of the

molecular beam and single crystal. In determining the reaction probability, a complication arises from the effusive hydrogen load on the main chamber. Since the crystal temperature is well below the onset of associative desorption for small hydrogen coverages, the effusive load from the expansion chamber leads to hydrogen adsorption prior to letting the molecular beam impinge onto the crystal. We have quantified H_2 adsorption prior to the actual measurement of S_0 using integrated TPD features with a full monolayer as reference. For all data presented here, the initial hydrogen coverage was less than 0.04 ML.

Using the described techniques, we have determined the reaction probability at a surface temperature of 300 K. We have also measured the reactivity between 100 and 300 K in steps of 50 K for Pt(211) and Pt(533), but we found no measurable differences from the data presented here. When going to higher surface temperatures, associative desorption starts competing with dissociative adsorption.

■ RESULTS AND DISCUSSION

HD Production from H_2 and D_2. We first present results from a series of experiments that produce HD from equally mixed H_2/D_2 supersonic molecular beams. Somorjai and co-workers performed similar experiments using effusive beams to show that stepped Pt surfaces produced HD whereas this was difficult to detect for Pt(111).[3,4] In our experiments, a supersonic molecular beam is expanded at room temperature to ensure that our W nozzle produces little HD prior to the molecular beam impacting onto the Pt-stepped surfaces. The lower half of Figure 3 shows the HD partial pressure in the UHV chamber. Here, the surface temperature of the Pt(211) surface ($n = 3$) is kept at 600 K, which is well above the associative desorption temperature of hydrogen from stepped and atomically flat platinum single-crystal surfaces.[38] At 450 K, we observe quantitatively the same results, but at 350 K, the HD production has dramatically reduced and is difficult to quantify. With time (bottom axis), we opened and closed an inert beam flag that intercepts the molecular beam in the UHV chamber at an upstream position relative to the sample. While the beam flag was closed, we rotated the crystal relative to the molecular beam in a direction nearly orthogonal to the steps. The top axis of Figure 3 shows the angle of incidence relative to the normal of the polished surface of the crystal at times when the H_2/D_2 beam impinged onto the stationary surface. The incident angles were −60°, −40°, −20°, 0°, 20°, 40°, and 60°. The increase in the HD partial pressure with increasing angle indicates that the overall kinetics resulting for H_2 (D_2) dissociative adsorption, H(D) diffusion, and H+D recombinative desorption are favorably influenced when H_2 and D_2 impact onto the surface with an approach direction into the open side of the step. We have performed the same experiment on Pt(533) and find the same general behavior although the overall reactivity is ~20% lower and the angle dependence of the HD production rate is slightly stronger.

The general shape of the reactivity compares well with results published by Somorjai's group.[5,6] They also showed that the angle of impact of the reactants affects overall reactivity. HD production continuously and smoothly increased by a factor of ~2 when rotating their Pt(332) sample with a (110) step type orthogonal to the step direction from −60° to +60° relative to the surface normal, with the highest reactivity observed when reactants impinged into the step. When taking the background
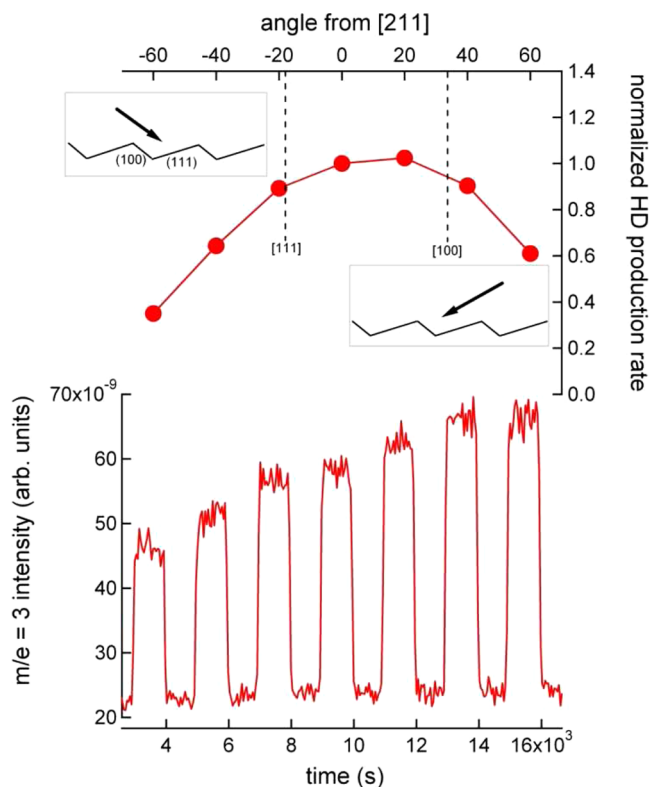
Figure 3. (top) Normalized rate of HD production as a function of incident angle of the reactants. (bottom) HD partial pressure in the UHV chamber while an H_2/D_2 supersonic beam expanded at room temperature is intermittently allowed to impinge onto Pt(211) at 600 K as a function of time while the sample was rotated in between exposures.

partial pressure into account, we also find an increase by a factor of ~2.

In the upper half of Figure 3, we indicate the [111] terrace and [100] step normals for our Pt(211) surface. Against the right axis, we again show the reactivity data at the indicated angles after subtracting the background signal and normalizing to the reactivity observed at incidence along the [211] direction, which we arbitrarily choose to be unity. Here, we have also corrected the data for the varying Pt surface area that the molecular beam impinges upon. By multiplying the measured HD production rate by cos θ, we account for the increasing number of Pt atoms available to partake in the entire catalytic process when rotating away from the surface normal, while keeping the number of H_2 and D_2 molecules entering the UHV chamber per second fixed. These data thus visualize how the average turnover frequency for surface platinum atoms in the H−D exchange reaction is affected by the approach angle of the reactants under the conditions of this experiment. It is asymmetric and highest in between the [211] and [100] directions. Our other Pt surfaces show the same behavior of having highest turnover frequencies when impinging molecules approach in between the surface normal and the [100] direction. It is likely that the asymmetry in the HD production is at least in part reflecting angle dependence in the dissociative adsorption probability. To obtain a more detailed understanding how atomic steps facilitate HD production on such Pt surfaces, we continue our investigation focusing on the initial elementary step, that is, the dissociative adsorption of molecular hydrogen and deuterium.

Dependence of S_0 on Angle of Impact and Kinetic Energy of the Incident Molecule.
The upper half of Figure 4 shows the angle dependence of the dissociation probability of
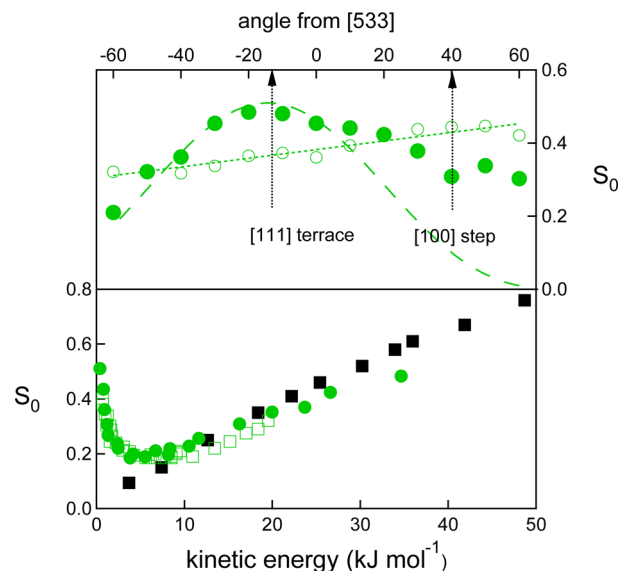

Figure 4. (top) Angle dependence of the reaction probability of hydrogen on Pt(533) with E_{kin} = 1.0 (open symbols) and 34 kJ/mol (solid symbols) and fits (see text for details). (bottom) Energy dependence of the reaction probability of hydrogen on Pt(533) as determined in our lab (green solid circles) and ref 20 (green open squares) and Pt(111) (solid squared).[23]

hydrogen on Pt(533) (n = 4). It shows absolute reaction probabilities in the zero-coverage limit (S_0) determined for two different incident energies (closed and open circles for ~1.0 and 34 kJ/mol, respectively) at a surface temperature of 300 K.

The sticking probability data shown here are representative of all three surfaces studied by us with minor differences. The low-energy data show a weak angle dependence that is reproduced rather well by a linear function (shown as a dotted line). Although the dependence seems weak, dissociation by the mechanisms operative at very low energies is favored by an approach angle that directs the hydrogen molecule into a step. From the angle-dependent results of our other Pt surfaces, we observe that this dependence on angle becomes somewhat steeper with decreasing step density. This indicates that, for a longer terrace, it becomes slightly more important to hit the step site at the appropriate angle. The fact that the angle dependence is observed up to angles of 60° is explained by the angles between the (100) and (111) plane, which is 55°, and the angle between the (533) and (111) plane, which is 14°. At an incident angle of +60° relative to the [533] normal, hydrogen molecules approach the crystal nearly parallel to the (111) terraces. McCormack et al. have suggested that a more grazing angle of incidence along the (111) plane may enhance trapping in the deep molecular chemisorption well that is present at the (100) step sites.[18]

For high incident energy, the angle dependence mostly reverses and becomes nonlinear. For all three surfaces studied, the reaction probability peaks near the [111] normal. The data in the near vicinity can be accurately modeled by a $\cos^3(\theta - \theta^{[111]})$ functional form, with $\theta^{[111]}$ being the absolute angle between the surface normal and the (111) terrace normal, as proposed by Gee et al.[20] However, we note that the direct

activated contribution to reactivity is not likely symmetrical over a wide angular range on stepped surfaces with short terraces. A more detailed analysis of our angle-dependent data is presented elsewhere.[39]

The lower half of Figure 4 shows the energy dependence of the sticking probability for Pt(533) with hydrogen (H_2 and D_2) incident along the macroscopic surface normal (green solid circles). It shows high dissociation probabilities at very low incident energies, lower values for S_0 at medium kinetic energies, and again higher values at the highest molecular speeds. Data published previously by Hayden and co-workers for the same Pt(533) surface are shown (green open squares).[20] Our data are in quantitative agreement up to 11 kJ/mol. We find slightly higher values for S_0 between 11 and 20 kJ/mol. The general trend is qualitatively consistent with the three distinct dissociation mechanisms suggested from the theoretical dynamics studies.[18] The initial drop in S_0 with kinetic energy is expected for an indirect, nonactivated mechanism. At high kinetic energies, S_0 increases linearly with kinetic energy. This behavior is expected for a direct activated mechanism that could occur on the 4 atom wide (111) terraces of the Pt(533) surface. Finally, extrapolation of the linear part of the reactivity at higher kinetic energies to zero kinetic energy yields an intercept well above the origin. This is consistent with the presence of a direct nonactivated reaction mechanism. For comparison, initial reaction probabilities determined for Pt(111)[23] are shown as black solid squares. This surface does not show the strong upturn in reactivity at the lowest kinetic energy that would be caused by the indirect nonactivated mechanism. Also, extrapolation of the reactivity to zero kinetic energy yields an intercept near zero, consistent with the absence of step sites where nonactivated direct adsorption could occur.

Separating Contributions to S_0 from Different Reactions Mechanisms. Figure 5 shows absolute reaction probabilities (S_0) for H_2 and D_2 on Pt(211). Here, we discriminate between H_2 (open red circles) and D_2 (solid red

circles). Although there is little data for the comparison of the isotopes at the lowest energies, we do not observe a significant isotope dependence in the entire kinetic energy range. Also, the general trend observed for Pt(533) in Figure 4 is repeated in Figure 5 for Pt(211). We conclude that the same dissociation mechanisms may be used to describe reactivity for both $n = 3$ and $n = 4$ in the class of $[n(111) \times (100)]$ surfaces.

We model the reactivity data with a functional form that represents contributions of the indirect nonactivated, the direct nonactivated, and the direct activated mechanisms, respectively. The functional form

$$S_0 = A \times e^{-\alpha \times E_{kin}} + B + C \times E_{kin} \tag{1}$$

reflects reasonable energy dependencies for the three dissociation mechanisms. In Figure 5, our best fit to the data is indicated as a solid red line. The individual contributions from the dissociation mechanisms are indicated as various dashed lines. The exponential decay (long dash), resulting from an increasing inability to absorb or transform kinetic energy of the impinging molecule to form a molecular precursor near the step, only contributes significantly at very low kinetic energies (<6 kJ/mol). The short length of the (211) unit cell, resulting in a relative large area of the upper edge of the step where impinging H_2 directly dissociates, is responsible for the large contribution of the direct nonactivated mechanism (short dash). Beyond kinetic energies of 25 kJ/mol, it is surpassed by the direct activated mechanism occurring on the short (111) terrace (dash-dot). We have previously compared our experimental results to predictions from six-dimensional quantum dynamics studies, concluding that the agreement was quantitatively reasonable.[21]

We have tested whether the same functional form accurately models reactivity data for the other stepped Pt surfaces. Figure 6 shows in the lower panel all S_0 data for Pt(211) (red solid circles), Pt(533) (green solid circles), and Pt(755) (blue solid
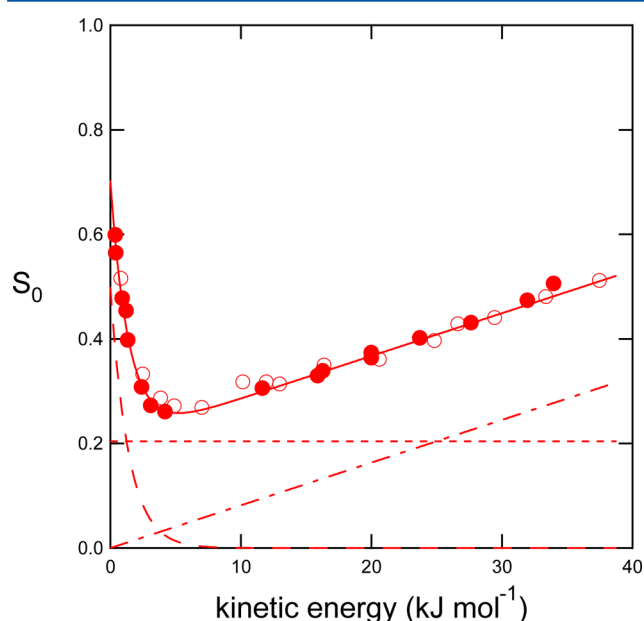
Figure 5. Absolute reaction probabilities for H_2 (open red circles) and D_2 (solid red circles) impacting along the macroscopic normal onto Pt(211). Lines represent the total (solid line) and mechanism-dependent (dashed lines) reactivities (see text for details).
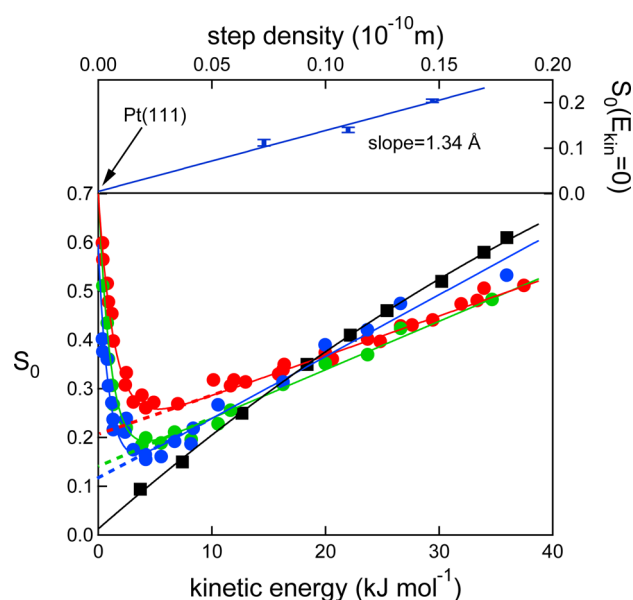
Figure 6. (top) Plot of parameter B^{hkl} vs step density with best unconstrained linear fit (solid line). (bottom) Kinetic energy dependence of the reaction probability of hydrogen for Pt(111) with polynomial fit (black solid squares and line),[23] Pt(211) (red solid circles), Pt(533) (green solid circles), and Pt(755) (blue solid circles) and best fits as described in the text (solid lines).

circles). Data for Pt(111) (solid black squares) are again included for reference. Although we do not show error bars for clarity, we have determined these by repeatedly measuring S_0 for each given set of conditions at least three times. The solid lines show the best fit of eq 1 to the data for each individual surface. For visual clarity, we also extrapolate the linear part of the fit as dotted lines toward zero kinetic energy to clearly show that the intercept B consistently drops in the following order: $B^{755} < B^{533} < B^{211}$.

From the parameters in eq 1, the most straightforward to interpret is B. It represents the fraction of incident molecules that dissociate upon impact at the upper edge of the step even when they have no significant amount of kinetic energy. In the absence of steering, it should reflect the fraction of the surface area of the unit cell where an impinging molecule encounters no barrier to dissociation nor requires a precursor state to dissociate. Theoretical dynamics studies have shown that steering is not significant for this system.[18,19] When we fit our experimental data for S_0 with the functional form presented in eq 1, we find three values for B^{hkl}. Plotted against step density, B^{hkl} should show a linear dependence as the number of molecules that react upon impact at a step scales linearly with step density. It should also approach zero for the (111) surface as that surface has no steps where nonactivated adsorption can take place. The top panel of Figure 6 shows our values of B^{hkl} versus step density ($Å^{-1}$) (top axis). The error bars reflect the uncertainties in B^{hkl} resulting from the least-squares fits to the reaction probability data in the bottom panel. The solid line in the top panel of Figure 6 is the best unconstrained linear fit through the data. Extrapolation to zero step density yields B^{111} = 0, in accordance with expectation.

The slope determined in the top panel of Figure 6 represents the average length of the unit cell (as measured orthogonal to the step direction) over which nonactivated direct dissociation occurs at the (100) step. When multiplying this average length of 1.34 ± 0.10 Å with the width of the unit cell (see gray shaded area in Figure 2 for reference), we obtain a surface area of 3.7 $Å^2$ that is available for nonactivated direct adsorption within the unit cell. A better interpretation of this value is to consider it the absolute reaction cross section for direct hydrogen dissociation at the top edge of the (100) step for incidence along the macroscopic surface normal. Also, this value of 3.7 $Å^2$ is obviously independent of unit cell length and compares to total unit cell areas of, for example, 18.8 and 25.2 $Å^2$ for Pt(211) and Pt(533), respectively.

We crudely estimate the same area from a cut through the PES reported by McCormack et al.[18] When we integrate the surface area where no barrier for direct dissociation is encountered from their calculations, we obtain 4.3 $Å^2$. Considering the crudeness of this comparison and the uncertainties in the exact height and location of reaction barriers obtained by DFT calculations, we consider this good agreement. Our ability to obtain an absolute reaction cross section for a dissociative adsorption mechanism is to the best of our knowledge unique in gas–surface reaction dynamics for molecules impinging onto a clean surface. However, it is related to absolute reaction cross sections determined for other gas–surface processes, for example, Eley–Rideal reactions of H atoms impinging onto surface-bound H atoms (e.g., see ref 40), noble-gas atoms "hammering" surface-bound H atoms into subsurface sites,[41,42] dissociating physisorbed CH_4 molecules on Ni(111) using inert-gas atoms,[43] and scattering cross

sections, for example, as we recently reported for H_2 scattering from a partially CO-covered Ru(0001) surface.[44]

General Predictive Model for Reactivity of Hydrogen on Platinum Surfaces. Next, we address whether a simple model can predict reaction probabilities for any value of the terrace length, n, using no more than the fit parameters as determined for Pt(211) where $n = 3$. The reactivity model is based on allocating the direct and indirect nonactivated mechanisms to the step and the direct activated mechanism to the terrace as described previously by McCormack et al.[18] They used this model to compare absolute reaction probabilities from dynamical simulations on Pt(211) ($n = 3$) to experimental results for Pt(533) ($n = 4$). The overall dissociation probability is the summation of these probabilities at the step and terrace:

$$S_{0,\text{total}}^{hkl} = S_{0,\text{step}}^{hkl} + S_{0,\text{terrace}}^{hkl} \tag{2}$$

As the size of the step does not vary between different unit cells, but the terrace length does, the separate contributions, normalized to the length of the unit cell, are described by

$$S_{0,\text{step}}^{hkl} = S_{0,hkl}^{211} \times \frac{L^{211}}{L^{hkl}} \tag{3}$$

$$S_{0,\text{terrace}}^{hkl} = S_{0,\text{terrace}}^{211} \times Q \times \frac{L^{211}}{L^{hkl}} \tag{4}$$

Here, L^{hkl} is the length of the (hkl) unit cell. Q is illustrated in Figure 7 and equals the relative expansion of the terrace length
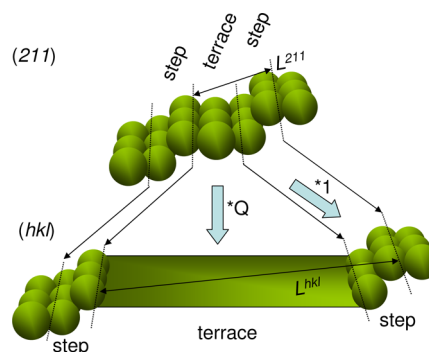

Figure 7. Schematic illustration of surface area changes in the unit cell that must be taken into account when comparing reactivity contributions from step and terrace for the (211) and (hkl) unit cells. The step size does not change whereas the terrace size is increased by a factor Q.

when comparing (211) to (hkl). The value of Q depends on the exact location of the boundaries between step and terrace as defined in the smallest, that is, the (211), unit cell. In Figure 7, they are indicated by dotted lines. From the perspective of the step edge, the boundaries are located such that they encompass nearly the entire first Pt atom at the higher terrace and most of the first Pt atom in the lower terrace. Obviously, this choice is arbitrary, and there are no general guidelines for the exact positioning of these boundaries. The most successful definition of Q for H_2/Pt as used by McCormack et al. located these boundaries such that the step encompasses ~55% or 10.2 $Å^2$ of the total surface area of the unit cell. The remaining ~45% or 8.6 $Å^2$ is considered (111) terrace.

Lacking in the model by McCormack et al. is the angle dependence known to exist for the activated dissociation

mechanism at the (111) terraces. We include this dependence and correct $S_{0\text{terrace}}$ in eq 3 by multiplying the righthand side terms with the ratio $\cos^m(\theta^{hkl} - \theta^{111})/\cos^m(\theta^{211} - \theta^{111})$. To obtain a reasonable value for m, we turn to angle-dependent sticking probabilities presented by Luntz et al.[23] The angle dependence for the direct activated dissociation mechanism on Pt(111) shows a complex behavior and is not represented over the entire angular and kinetic energy ranges by a single value of m. However, we have reanalyzed those data for the most appropriate available off-normal angle (i.e., 30°) and find that $m = 1.4$ yields the best fit between 0 and 40 kJ/mol. As the angle dependence in the low kinetic energy regime, where steps dominate reactivity, was weak for all surfaces, we apply no correction to $S_{0,\text{step}}$.

Figure 8 compares the predictions from our model to experimentally determined reaction probabilities for various
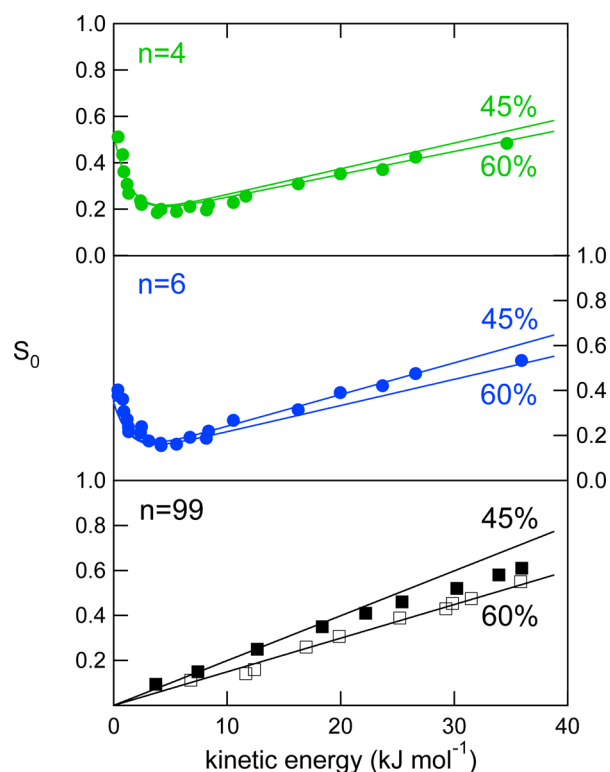

Figure 8. Experimental data (solid symbols) and predictions (lines) for the dissociation probability of hydrogen on Pt(533) (top, green), Pt(755) (middle, blue), and Pt(111) (bottom, black). Experimental data for Pt(533) and Pt(755) are the same as in Figure 6. Data for Pt(111) are taken from ref 23 (solid circles) and ref 24 (open circles).

$\text{Pt}[n(111) \times (100)]$ surfaces. The experimental data are shown as symbols. For $n = 4$, that is, Pt(533), we only show our own data as data obtained by Hayden's group[20] (shown in Figure 4) are mostly in quantitative agreement. The data for $n = 6$, that is, Pt(755), were also obtained in our group. The data for Pt(111) are taken from Luntz et al.[23] and Samson et al.[24] The predictions from our model, based on the parameters obtained from the fit to the data for Pt(211) in Figure 5, are shown as solid lines in Figure 8. We have used two limiting values of Q. These are determined from relating at least 45% and at most 60% of the (211) surface area to terrace reactivity with the remainder belonging to step reactivity. Note that, for the comparison to Pt(111), we use $n = 99$ in our model. This

approximates a realistic value for Pt(111) surfaces with a miscut on the order of 1°. Predictions for much larger values of n (corresponding to smaller miscuts) are not noticeably different from the predictions shown here.

The comparison in Figure 8 leads us to conclude that all experimental data from supersonic molecular beam studies published to date are accurately predicted by our simple model and we have successfully separated and quantified the absolute reactivity of step sites and terrace sites for this elementary reaction. It required no more than fit parameters determined from data for $n = 3$ and any value of Q based on a (111) terrace size equal to 45–60% of the surface area of the (211) unit cell. In this regard, it is noteworthy that we did not need to include the weakly bound molecular state for the (111) terrace that was recently suggested by Poelsema and co-workers.[25] A simple model based on a molecular adsorption well for H_2 on (111) terraces and a surface-temperature-dependent diffusion length across the (111) surface quantitatively explained both adsorption and desorption data on their nearly defect-free Pt(111) surface. Dissociation was entirely accounted for and attributed to the extremely low defect concentration. At our experimental conditions, with a surface temperature of 300 K in most experiments, this precursor state is very short-lived. Its diffusion length is estimated to be on the order of atomic distances. As for a thermalized gas at ~300 K, Poelsema and co-workers found an energy- and impact-angle-averaged dissociation probability of 0.05 resulting from this precursor state at a surface temperature of 155 K; the contribution of this dissociation mechanism in our experiments is insignificant. Also, in further studies, Poelsema and co-workers created hexagonally shaped islands and wells on Pt(111).[26] They found an additional dissociation mechanism whose contribution to the dissociation probability was directly proportional to step density. This is fully in agreement with our findings that, at very low impact energies, reactivity can be entirely accounted for by dissociation at steps. A more detailed comparison is difficult as the hexagonal Pt islands in their study contain both (111) and (100) step types and their data was obtained without kinetic or angular resolution.

We conclude that our measurements and model establish for the first time that theoretical studies of the smallest unit cell, which includes a particular step type, suffice to predict reactivity for any unit cell of the same type. This finding is crucial to accurate kinetic modeling of catalytic reactions as, for general cases, it requires knowledge of the site-dependent reactivity on catalytic surfaces. As mentioned, barrier heights for dissociative adsorption at steps, which are used as input for kinetic models, are generally based on DFT calculations for fcc(211) or comparable small unit cells.[45] Our findings provide the first independent experimental support for this simplification. However, they also point toward conditions that restrict this assumption. The following are required:

(1) A detailed understanding of all reaction pathways contributing to dissociation and their energy dependencies.

(2) A strict separation between reaction at step and terrace sites for all mechanisms that contribute significantly.

(3) An accurate estimate of the surface areas within the smallest unit cell that contribute to step and terrace reactivity.

The first and second conditions suggest that at least quasi-classical dynamics studies of dissociation on the smallest

representative unit cell are required to establish which reaction mechanisms may be of relevance and to what extent they are separable. The second condition is explicitly required as the occurrence of long-lived (chemi- or physisorbed) precursor states, which enable diffusion over significant distances, will annihilate the strict relation between site of impact and site of reaction. Poelsema, Lenz, and Comsa proposed such a state in an alternative description of H_2 dissociation on Pt(111).[25,26] However, this mechanism does not contribute significantly at surface temperatures considered here. The third requirement must be met for accurate scaling between $n = 3$ and any other value. We have recently shown that the separate contributions to reactivity occurring at steps and terraces in combination with Wulff constructions of nanoparticles and simple kinetic models allow us to predict under which pressure and temperature circumstances dissociation occurs mostly at steps versus terraces.[8]

CONCLUSIONS

Summarizing, we present the first systematic study of hydrogen dissociation dynamics on stepped Pt surfaces using supersonic molecular beam techniques. All our data for three different stepped surfaces of the type $[n(111) \times (100)]$ regarding HD production from H_2/D_2 beams and angle, surface temperature, and kinetic energy dependencies are in line with three separate mechanisms for dissociation proposed by previous high-dimensionality theoretical studies. A simple fit to reactivity data for the smallest stepped unit cell accounting for these three independent dissociation pathways allows us to accurately predict hydrogen dissociation for any Pt surface containing (100) steps and (111) terraces. We thereby separate and quantify the absolute reactivity for edges and terraces occurring on real catalytic particles. Our ability to do so provides support for crucial simplifications used in theoretical predictions of reaction kinetics and sets guidelines for incorporation of surface defect influences in such studies. Finally, it provides a means to extract previously unattainable absolute reaction cross sections in gas–surface dynamics studies.

AUTHOR INFORMATION

Corresponding Author
*Phone: +31 71 527 4221; e-mail: l.juurlink@chem.leidenuniv.nl.

Notes
The authors declare no competing financial interest.

ACKNOWLEDGMENTS

REFERENCES

(1) Ertl, G. Reactions at Surfaces: From Atoms to Complexity (Nobel Lecture). *Angew. Chem., Int. Ed.* **2008**, *47*, 3524–3535.
(2) Somorjai, G. A.; Li, Y. M. Impact of Surface Chemistry. *Proc. Natl. Acad. Sci. U.S.A.* **2011**, *108*, 917–924.
(3) Bernasek, S. L.; Siekhaus, W. J.; Somorjai, G. A. Molecular-Beam Study of Hydrogen-Deuterium Exchange on Low-Miller-Index Platinum Single-Crystal Surfaces. *Phys. Rev. Lett.* **1973**, *30*, 1202–1204.

(4) Bernasek, S. L.; Somorjai, G. A. Molecular Beam Study of Mechanism of Catalyzed Hydrogen-Deuterium Exchange on Platinum Single-Crystal Surfaces. *J. Chem. Phys.* **1975**, *62*, 3149–3161.
(5) Gale, R. J.; Salmeron, M.; Somorjai, G. A. Variation of Surface-Reaction Probability with Reactant Angle of Incidence: A Molecular Beam Study of Asymmetry of Stepped Platinum Crystal Surfaces for H-H Bond Breaking. *Phys. Rev. Lett.* **1977**, *38*, 1027–1029.
(6) Salmeron, M.; Gale, R. J.; Somorjai, G. A. Molecular-Beam Study of H_2–D_2 Exchange-Reaction on Stepped Platinum Crystal Surfaces: Dependence of Reactant Angle of Incidence. *J. Chem. Phys.* **1977**, *67*, 5324–5334.
(7) Salmeron, M.; Gale, R. J.; Somorjai, G. A. Modulated Molecular-Beam Study of the Mechanism of the H_2–D_2 Exchange-Reaction on Pt(111) and Pt(332) Crystal Surfaces. *J. Chem. Phys.* **1979**, *70*, 2807–2818.
(8) Groot, I. M. N.; Kleyn, A. W.; Juurlink, L. B. F. The Energy Dependence of the Ratio of Step and Terrace Reactivity for H_2 Dissociation on Stepped Platinum. *Angew. Chem., Int. Ed.* **2011**, *50*, 5174–5177.
(9) Vattuone, L.; Savio, L.; Rocca, M. Bridging the Structure Gap: Chemistry of Nanostructured Surfaces at Well-Defined Defects. *Surf. Sci. Rep.* **2008**, *63*, 101–168.
(10) Norskov, J. K.; Abild-Pedersen, F.; Studt, F.; Bligaard, T. Density Functional Theory in Surface Chemistry and Catalysis. *Proc. Natl. Acad. Sci. U.S.A.* **2011**, *108*, 937–943.
(11) Norskov, J. K.; Bligaard, T.; Hvolbaek, B.; Abild-Pedersen, F.; Chorkendorff, I.; Christensen, C. H. The Nature of the Active Site in Heterogeneous Metal Catalysis. *Chem. Soc. Rev.* **2008**, *37*, 2163–2171.
(12) Vanhove, M. A.; Somorjai, G. A. New Microfacet Notation for High-Miller-Index Surfaces of Cubic Materials with Terrace, Step and Kink Structures. *Surf. Sci.* **1980**, *92*, 489–518.
(13) Hellman, A.; Honkala, K.; Remediakis, I. N.; Logadottir, A.; Carlsson, A.; Dahl, S.; Christensen, C. H.; Norskov, J. K. Ammonia Synthesis and Decomposition on a Ru-Based Catalyst Modeled by First-Principles. *Surf. Sci.* **2009**, *603*, 1731–1739.
(14) Honkala, K.; Hellman, A.; Remediakis, I. N.; Logadottir, A.; Carlsson, A.; Dahl, S.; Christensen, C. H.; Norskov, J. K. Ammonia Synthesis from First-Principles Calculations. *Science* **2005**, *307*, 555–558.
(15) Jones, G.; Jakobsen, J. G.; Shim, S. S.; Kleis, J.; Andersson, M. P.; Rossmeisl, J.; Abild-Pedersen, F.; Bligaard, T.; Helveg, S.; Hinnemann, B.; et al. First Principles Calculations and Experimental Insight into Methane Steam Reforming over Transition Metal Catalysts. *J. Catal.* **2008**, *259*, 147–160.
(16) Grabow, L. C.; Studt, F.; Abild-Pedersen, F.; Petzold, V.; Kleis, J.; Bligaard, T.; Norskov, J. K. Descriptor-Based Analysis Applied to HCN Synthesis from NH_3 and CH_4. *Angew. Chem., Int. Ed.* **2011**, *50*, 4601–4605.
(17) Van Hardeveld, R.; Van Montoort, A. Influence of Crystallite Size on Adsorption of Molecular Nitrogen on Nickel, Palladium and Platinum: An Infrared and Electron-Microscopic Study. *Surf. Sci.* **1966**, *4*, 396–430.
(18) McCormack, D. A.; Olsen, R. A.; Baerends, E. J. Mechanisms of H_2 Dissociative Adsorption on the Pt(211) Stepped Surface. *J. Chem. Phys.* **2005**, *122*, 044701.
(19) Olsen, R. A.; McCormack, D. A.; Luppi, M.; Baerends, E. J. Six-Dimensional Quantum Dynamics of H_2 Dissociative Adsorption on the Pt(211) Stepped Surface. *J. Chem. Phys.* **2008**, *128*, 194715.
(20) Gee, A. T.; Hayden, B. E.; Mormiche, C.; Nunney, T. S. The Role of Steps in the Dynamics of Hydrogen Dissociation on Pt(533). *J. Chem. Phys.* **2000**, *112*, 7660–7668.
(21) Groot, I. M. N.; Schouten, K. J. P.; Kleyn, A. W.; Juurlink, L. B. F. Dynamics of Hydrogen Dissociation on Stepped Platinum. *J. Chem. Phys.* **2008**, *129*, 224707.
(22) Nieto, P.; Pijper, E.; Barredo, D.; Laurent, G.; Olsen, R. A.; Baerends, E. J.; Kroes, G. J.; Farias, D. Reactive and Nonreactive Scattering of H_2 from a Metal Surface is Electronically Adiabatic. *Science* **2006**, *312*, 86–89.

(23) Luntz, A. C.; Brown, J. K.; Williams, M. D. Molecular-Beam Studies of H_2 and D_2 Dissociative Chemisorption on Pt(111). *J. Chem. Phys.* **1990**, *93*, 5240−5246.

(24) Samson, P.; Nesbitt, A.; Koel, B. E.; Hodgson, A. Deuterium Dissociation on Ordered Sn/Pt(111) Surface Alloys. *J. Chem. Phys.* **1998**, *109*, 3255−3264.

(25) Poelsema, B.; Lenz, K.; Comsa, G. The Dissociative Adsorption of Hydrogen on Defect-'Free' Pt(111). *J. Phys.: Condens. Mat.* **2010**, *22*, 304006.

(26) Poelsema, B.; Lenz, K.; Comsa, G. The Dissociative Adsorption of Hydrogen on Pt(111): Actuation and Acceleration by Atomic Defects. *J. Chem. Phys.* **2011**, *134*, 074703.

(27) Riedmüller, B.; Giskes, F.; van Loon, D. G.; Lassing, P.; Kleyn, A. W. A Compact Molecular Beam Line. *Meas. Sci. Technol.* **2002**, *13*, 141−149.

(28) Backus, E. H. G.; Eichler, A.; Grecea, M. L.; Kleyn, A. W.; Bonn, M. Adsorption and Dissociation of NO on Stepped Pt(533). *J. Chem. Phys.* **2004**, *121*, 7946−7954.

(29) Gohndrone, J. M.; Masel, R. I. A TPD Study of Nitric-Oxide Decomposition on Pt(100), Pt(411) and Pt(211). *Surf. Sci.* **1989**, *209*, 44−56.

(30) Mukerji, R. J.; Bolina, A. S.; Brown, W. A. An Investigation of the Effect of Pre-Dosed O Atoms on the Adsorption of NO on Pt{211}. *Surf. Sci.* **2003**, *547*, 27−44.

(31) Mukerji, R. J.; Bolina, A. S.; Brown, W. A. The Influence of Steps on the Dissociation of NO on Pt Surfaces: Temperature-Programmed Desorption Studies of NO Adsorption on Pt{211}. *J. Chem. Phys.* **2003**, *119*, 10844−10852.

(32) Mukerji, R. J.; Bolina, A. S.; Brown, W. A. A RAIRS and TPD Investigation of the Adsorption of CO on Pt{211}. *Surf. Sci.* **2003**, *527*, 198−208.

(33) Sugisawa, T.; Shiraishi, J.; Machihara, D.; Irokawa, K.; Miki, H.; Kodama, C.; Kuriyama, T.; Kubo, T.; Nozoye, H. Adsorption and Decomposition of NO on Pt(112). *Appl. Surf. Sci.* **2001**, *169*, 292−295.

(34) Xu, J. Z.; Yates, J. T. Terrace Width Effect on Adsorbate Vibrations: A Comparison of Pt(335) and Pt(112) for Chemisorption of CO. *Surf. Sci.* **1995**, *327*, 193−201.

(35) Ellis, W. P.; Schwoebel, R. L. LEED from Surface Steps on UO_2 Single Crystals. *Surf. Sci.* **1968**, *11*, 82−98.

(36) Henzler, M. LEED-Investigations of Step Arrays on Cleaved Germanium (111) Surfaces. *Surf. Sci.* **1970**, *19*, 159−171.

(37) King, D. A.; Wells, M. G. Reaction-Mechanism in Chemisorption Kinetics: Nitrogen on {100} Plane of Tungsten. *Proc. R. Soc. London,. Ser. A* **1974**, *339*, 245−269.

(38) Lu, K. E.; Rye, R. R. Flash Desorption and Equilibration of H_2 and D_2 on Single-Crystal Surfaces of Platinum. *Surf. Sci.* **1974**, *45*, 677−695.

(39) Groot, I. M. N. *The Fight for a Reactive Site*; Leiden University: Leiden, The Netherlands, 2009.

(40) Tully, J. C. Chemical Dynamics at Metal Surfaces. *Annu. Rev. Phys. Chem.* **2000**, *51*, 153−178.

(41) Kindt, J. T.; Tully, J. C. Simulations of Collision-Induced Absorption of Hydrogen on Ni(111). *J. Chem. Phys.* **1999**, *111*, 11060−11069.

(42) Maynard, K. J.; Johnson, A. D.; Daley, S. P.; Ceyer, S. T. A New Mechanism for Absorption: Collision-Induced Absorption. *Faraday Discuss.* **1991**, *91*, 437−449.

(43) Beckerle, J. D.; Johnson, A. D.; Yang, Q. Y.; Ceyer, S. T. Collision-Induced Dissociative Chemisorption of CH_4 on Ni(111) by Inert-Gas Atoms: The Mechanism for Chemistry with a Hammer. *J. Chem. Phys.* **1989**, *91*, 5756−5777.

(44) Ueta, H.; Groot, I. M. N.; Gleeson, M. A.; Stolte, S.; McBane, G. C.; Juurlink, L. B. F.; Kleyn, A. W. CO Blocking of D_2 Dissociative Adsorption on Ru(0001). *ChemPhysChem* **2008**, *9*, 2372−2378.

(45) Rostrup-Nielsen, J.; Norskov, J. K. Step Sites in Syngas Catalysis. *Top. Catal.* **2006**, *40*, 45−48.